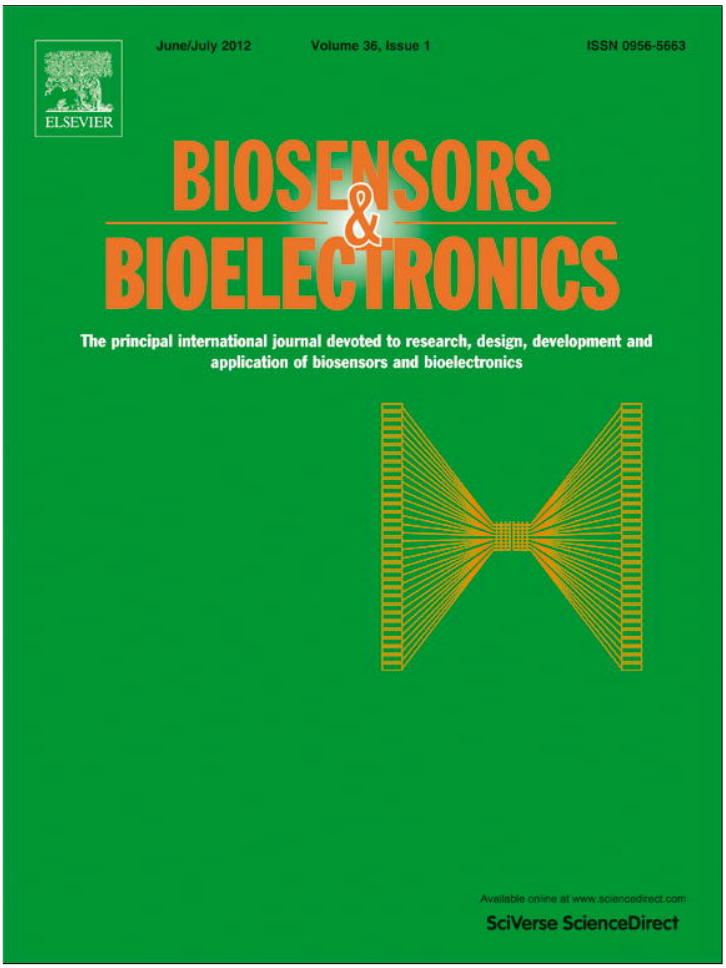

Biosensors and Bioelectronics 36 (2012) 12–17

Contents lists available at SciVerse ScienceDirect

Biosensors and Bioelectronics

journal homepage: www.elsevier.com/locate/bios

A simple electrochemical aptasensor for ultrasensitive protein detection using cyclic target-induced primer extension

Wei Cheng [a,b,1], Shijia Ding [a,1], Qing Li [a], Tianxiao Yu [a], Yibin Yin [a], Huangxian Ju [a,c,*], Guosheng Ren [b,**]

[a] Key Laboratory of Laboratory Medical Diagnostics—Ministry of Education of China, Department of Laboratory Medicine, Chongqing Medical University, Chongqing 400016, PR China
[b] Molecular Oncology and Epigenetics Laboratory, The First Affiliated Hospital of Chongqing Medical University, Chongqing 400016, PR China
[c] State Key Laboratory of Analytical Chemistry for Life Science, Department of Chemistry, Nanjing University, Nanjing 210093, PR China

ARTICLE INFO

Article history:
Received 2 January 2012
Received in revised form
1 March 2012
Accepted 16 March 2012
Available online 7 April 2012

Keywords:
Electrochemical biosensor
Aptasensor
Signal amplification
Primer extension
Protein
Ultrasensitivity

ABSTRACT

A simple electrochemical aptasensor was developed for ultrasensitive protein detection by combining a novel strategy of cyclic target-induced primer extension (CTIPE) with an aptamer-hairpin probe and enzyme-amplified electrochemical readout. In the presence of protein target, the immobilized aptamer-hairpin probe recognized the protein to trigger primer extension reaction by target-induced conformational transition, which released the protein from replicated DNA duplex. The released target could cyclically bind with other aptamer-hairpin probes and trigger new primer extension, leading to formation of numerous biotin-tagged DNA duplex, which significantly amplified the protein recognition event and facilitated the subsequent enzymatic signal enhancement, leading to an ultrasensitive electrochemical aptasensor. Using human vascular endothelial growth factor as a model protein, the designed aptasensor could detect protein down to 0.82 pg mL^{-1} with a linear range from 1 pg mL^{-1} to 1 ng mL^{-1}. The proposed aptasensor was amenable to quantification of protein in complex biological matrixes, and would become a simple and powerful tool for bioanalysis and clinic diagnostic application.

1. Introduction

The quantitative detection of protein biomarkers in body fluids or tissues plays essential roles in various molecular and cellular researches, as well as clinical diagnostics. Biosensing system offers an important alternative to the classical analytical methods for proteins detection (D'Orazio, 2011).

Biosensors using aptamer as a recognition element (aptasensor) have become promising techniques due to the advantages of aptamer over traditional antibody, such as high specificity and affinity, and good chemical stability, availability and flexibility (Ellington and Szostak, 1990; Tombelli et al., 2005; Liu et al., 2009). Numerous aptasensors have been proposed for detection of certain protein biomarkers by chemiluminescence (Li et al., 2010), electrochemistry (Hianik and Wang, 2009), fluorescence (Qiu et al., 2011), quartz crystal microbalance (Hianik et al., 2007), surface plasmon resonance (Wang and Zhou, 2008), and magnetic resonance imaging (Perez et al., 2002). Among them, the electrochemical aptasensors have received more attention due to their convenient miniaturization, simple preparation, rapid response and low cost (Sassolas et al., 2009; Xu et al., 2009). Although many reagentless and/or renewable electrochemical aptasensors have been explored for simple and rapid detection of proteins using impedance-based assays (Peng et al., 2009), target-induced conformational change (Lai et al., 2007) and target-induced strand displacement strategies (Zuo et al., 2007; Yoshizumi et al., 2008), and a series of nanomaterials, such as carbon nanotubes (Kara et al., 2010), gold nanoparticle (Wang et al., 2009; Kuang et al., 2010), magnetic nanobeads (Cheng et al., 2010a,b), quantum dots (Zhou et al., 2010) and other metal nanomaterials (Bai et al., 2011; Li et al., 2011), have been applied to enhance recognition events of targets and lower the detection limit, the variability of the nanomaterials and their bio-functionalization often affect the reproducibility and quantification of these aptasensors, especially for the real samples (Zhang et al., 2007). Thus, extensive effort is still an urgent demand to improve the sensitivity of electrochemical aptasensors.

Recently, rolling circle amplification (RCA) has been used in aptamer-based assays for signal amplification (Zhao et al., 2008). This isothermal DNA amplification technique is highly compatible to aptamer systems and does not require thermal cycling or special laboratory conditions (Lee et al., 2010). The aptamer-based (Zhou et al., 2007; Lee et al., 2010) or aptamer-initiated

* Corresponding author at: Key Laboratory of Laboratory Medical Diagnostics—Ministry of Education of China, Department of Laboratory Medicine, Chongqing Medical University, Chongqing 400016, PR China.
Tel./fax: +86 25 83593593.
** Corresponding author.
E-mail addresses: hxju@nju.edu.cn (H. Ju), rgs726@163.com (G. Ren).
[1] These authors contributed equally to this work.

0956-5663/$ - see front matter © 2012 Elsevier B.V. All rights reserved.
http://dx.doi.org/10.1016/j.bios.2012.03.032

(Cheng et al., 2010a,b) RCA strategies can significantly improve the sensitivity with the detection limits as low as 10 fM. However, their analytical procedures are complicated with the preparation of circular DNA templates. Thus isothermal strand-displacement polymerization has been applied in fluorescent aptasensor for signal amplification without especial preparation of circular DNA templates (He et al., 2010; Qiu et al., 2011). This technique can transfer the target-aptamer binding into the cyclic nucleic acid strand displacement polymerization. Unfortunately, a conspicuous blank fluorescence signal counteracts the signal amplification capability, compromising the analytical performance of the designed aptasensor (Qiu et al., 2011).

This work combined a novel cyclic target-induced primer extension (CTIPE) strategy with an immobilized aptamer-hairpin probe and enzymatic signal enhancement to develop a simple electrochemical aptasensor for ultrasensitive detection of protein. Human vascular endothelial growth factor (VEGF), an important angiogenic biomarker for tumor growth and metastasis (Ferrara et al., 2003; Prabhulkar et al., 2009), was employed as a model protein. The proposed aptasensor appeared excellent analytical performance toward protein detection, which provided a powerful and convenient platform for bioanalysis and clinic diagnostic application.

2. Materials and methods

2.1. Reagents

Streptavidin-alkaline phosphatase (ST-AP), 6-mercapto-1-hexanol (MCH), α-naphthyl phosphate (α-NP), bovine serum albumin (BSA) and salmon sperm DNA were purchased from Sigma-Aldrich (USA). Recombinant human VEGF was purchased from Bio Basic Inc. (Canada). Phi29 DNA polymerase and dNTP mixture were obtained from Fermentas (Lithuania). The enzyme-immunoassay kit for VEGF was purchased from Boster Biological Technology Co., Ltd. (China). All other reagents were of analytical grade. All aqueous solutions were prepared using ultra-pure water (≥ 18 MΩ, Milli-Q, Millipore). The oligonucleotides with the following sequences were obtained from Shanghai Sangon Biological Engineering Technology and Services Co., Ltd. (China):

aptamer-hairpin probe 1: 5′-thiol-$(CH_2)_6$-AAA AAA AAA A**CC GTC TTC CAG ACA AGA GTG CAG GG**A AAA AGA AGA CGG-3′;
aptamer-hairpin probe 2: 5′-**CCG TCT TCC AGA CAA GAG TGC AGG G**TT TTT TTG AAG ACG GTT TTT TT-thiol-$(CH_2)_6$-3′;
biotinylated primer: 5′-biotin-CCG TCT TC-3′.

The boldfaced regions indicate the aptamer sequences for VEGF (Potty et al., 2009), while the underlined regions indicate the complementary sequences for hairpin formation and primer hybridization.

2.2. Apparatus

All electrochemical measurements were performed on a CHI660D electrochemical analyzer (CHI Co., TX) with a conventional three-electrode system composed of platinum wire as auxiliary, Ag/AgCl electrode as reference, and a gold electrode (GE) as working electrode. Surface plasmon resonance (SPR) analysis was carried out using a BIACORE X instrument (Biacore AB, Sweden).

2.3. Preparation of electrochemical aptasensor

A gold electrode (GE) was polished with 0.05 μm alumina slurries and ultrasonically treated in deionized water. The electrode was then soaked in piranha solution (H_2SO_4:H_2O_2=3:1) for 10 min followed by rinsing thoroughly with deionized water to eliminate other substances. 10 μL of 400 nM thiolated aptamer-hairpin probe was dropped on the pretreated electrode surface and incubated overnight at 4 °C. The resulting electrode was immersed into 100 μL of 1 mM MCH solution for 1 h to occupy the left bare sites on electrode surface and obtain well-aligned DNA monolayer. The obtained electrochemical aptasensor was rinsed with ethanol and deionized water and used for following operation.

2.4. Protein detection protocol

Prior to use, the prepared electrochemical aptasensor was further soaked in 0.1 M pH 7.4 Tris–HCl buffer containing 125 μg mL^{-1} salmon sperm DNA and 2% BSA for 30 min to block the nonspecific binding sites on its surface, and rinsed with 0.1 M pH 7.4 Tris–HCl buffer containing 0.05% Tween 20. 10 μL of target analyte at variable concentrations was then dropped on the aptasensor surface and incubated for 1 h at 37 °C to form the VEGF-aptamer complex followed by rinsing thoroughly with pH 7.4 phosphate buffer saline (PBS, 136.7 mM NaCl, 2.7 mM KCl, 8.72 mM Na_2HPO_4 and 1.41 mM KH_2PO_4) containing 0.05% Tween 20. CTIPE reaction was performed by adding 10 μL CTIPE reaction mixture (0.2 units of phi29 DNA polymerase, 100 nM biotinylated primer, 1 mM dNTP 10 mM magnesium acetate, 33 mM potassium acetate, 1 mM dithiothreitol in 50 mM pH 7.5 Tris–HCl buffer) on the aptasensor surface and incubated at 37 °C for 1 h. After washing with PBS containing 0.05% Tween 20, the aptasensor was reacted with 10 μL of 1.25 μg mL^{-1} ST-AP in pH 9.6 diethanolamine buffer at 37 °C for 30 min, and washed thoroughly with diethanolamine buffer containing 0.05% Tween 20. Electrochemical measurement was then performed in pH 9.6 diethanolamine buffer containing 1 mg mL^{-1} of α-NP (Carpini et al., 2004). The differential pulse voltammetric (DPV) measurement was performed from 0 to 0.6 V with pulse amplitude of 50 mV and width of 50 ms.

2.5. SPR characterization of aptasensor fabrication

For SPR characterization, the aptamer-hairpin probe/MCH modified sensor chip was prepared with the similar process of aptasensor preparation. Briefly, the bare gold sensor chip was firstly cleaned with piranha solution for 5 min and rinsed with deionized water. The chip was then incubated in 400 nM thiolated aptamer-hairpin probe solution overnight at 4 °C, immersed into 100 μL of 1 mM MCH solution for 1 h and rinsed with ethanol and deionized water to obtain aptamer-hairpin probe/MCH modified sensor chip. SPR experiment was performed at 25 °C in pH 7.4 PBS contained 0.05% Tween 20 as a running buffer with a flow rate of 5 μL per minute After the sensorgram reached a stable baseline, 1 nM VEGF in PBS was passed over the sensor chip for 15 min followed by equilibrating with the running buffer. Then CTIPE reaction was performed on chip surface by passing CTIPE reaction mixture for 15 min and washing with running buffer. 5 mg mL^{-1} ST-AP was passed over the sensor chip for 15 min to bind ST-AP to the CTIPE product. The real-time result was displayed as a time course of resonance units (RU).

3. Results and discussion

3.1. Design of electrochemical aptasensor

The designed electrochemical aptasensor and CTIPE strategy are conceptually depicted in Fig. 1. Aptamer-hairpin probe containing aptamer sequence for VEGF, which could form loop-stem structure to block the primer hybridization, was immobilized on

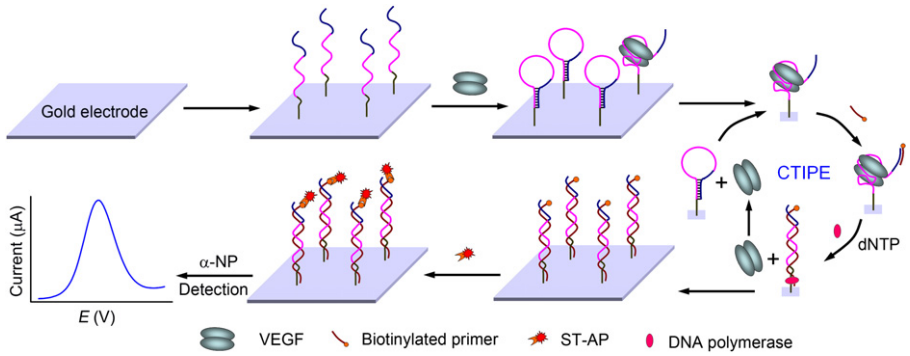

Fig. 1. Schematic presence of electrochemical aptasensor based on cyclic target-induced primer extension.

GE surface. The specific binding of VEGF to aptamer region changed the conformation of hairpin probe and opened the site for primer hybridization. In presence of nucleotides and DNA polymerase, the hybridization of biotinylated-primer triggered primer extension reaction. The protein target was then released by the replication of DNA duplex, and bound with other aptamer-hairpin probe, which led to new primer extension. So, the CTIPE system was run by a cyclic process of target binding, primer extension, target releasing and repeated binding. The designed CTIPE strategy could transfer single target-aptamer binding event into cyclic primer extension process to form a lot of biotin-tagged DNA duplex. ST-AP was then labeled on the CTIPE product by the specific recognition of AT and biotin, and the bound AP produced enzymatic signal enhancement. Dual signal amplification of CTIPE and enzymatic catalysis resulted in a simple electrochemical aptasensor for ultrasensitive detection of target protein.

3.2. Characterization of aptasensor fabrication

Electrochemical characteristics of aptasensor fabrication were obtained by cyclic voltammetry (CV) and electrochemical impedance spectroscopy (EIS). The cyclic voltammograms of $[Fe(CN)_6]^{3-/4-}$ solution at different modified electrodes were shown in Fig. 2A. The peak current decreased clearly after aptamer-hairpin probe was assembled on the GE surface, indicating that the assembled oligonucleotides severely hindered the diffusion of ferricyanide toward the electrode surface. Subsequently, when MCH was used to block residual active sites on GE surface and made the assembled DNA strands "stand up", the peak current further decreased due to electrostatic repulsion between the net negative dipole of the alcohol terminus on the gold surface and the negatively charged ferricyanide (Zhang et al., 2010). After the prepared aptasensor incubated with VEGF, a dramatically decrease in current was observed, indicating successful recognition and binding of target protein by the assembled aptamer-hairpin probe. These results were in a good agreement with those obtained from EIS (Fig. 2B), in which the surface electron transfer resistance increased upon the assembly and binding processes.

The stepwise reactions on the aptasensor were also characterized by real-time SPR sensorgram of the aptamer-hairpin probe/MCH modified chip (Fig. 2C). The SPR response showed the increase of RU after incubation with VEGF, further proved effective binding of target protein to aptamer-hairpin probe. For kinetic studies, the data were analyzed with BIAevaluation software (version 4.1) provided by the manufacturer. The dissociation constant (K_d) of VEGF/aptamer-hairpin probe complex was calculated to be 58.6 nM in PBS, indicating sufficient affinity of aptamer-hairpin probe to VEGF, though which was slightly lower than that obtained by previous report (Potty et al., 2009) due to the modified nucleotides at aptamer extremities. Subsequently, after CTIPE reaction was performed on chip surface the SPR response decreased slightly owing to the transition of VEGF/aptamer complex to DNA duplex. The final binding of ST-AP with biotin-tagged DNA duplex recovered the SPR response and resulted in remarkable increase of RU. These results demonstrated the successful implementation of CTIPE on chip surface and the feasibility of designed method.

3.3. Signal amplification performance of CTIPE

As shown in Fig. 3, the DPV curves of designed aptasensor showed a well-defined oxidation peak for target protein detection, which corresponded to the oxidation of α-naphthyl, the AP-catalyzed product of α-NP (Carpini et al., 2004). To demonstrate the designed CTIPE strategy and test its signal amplification, a CTIPE-free method was designed as a control. The DPV signal corresponding to 100 pg mL^{-1} VEGF showed remarkable increase with the introduction of CTIPE (curves c and d), indicating the cyclic process of the designed system formed a lot of biotin-tagged DNA duplex for signal amplification. After subtracting the response to blank solution, the peak current obtained with CTIPE strategy was about 6 times as much as that obtained with CTIPE-free control, showing remarkable amplification performance. A slight increase of DPV signal for blank solution was observed with CTIPE (curves a and b). This was likely attributed to a weak hybridization of hairpin-probe and primer, which resulted in a little part of the replication.

3.4. Optimization of aptasensor preparation and detection conditions

The formation of aptamer-hairpin probe affected intensely target binding and CTIPE process. Two aptamer-hairpin probes with different assembly orientation and primer hybridization position were tested, and their sensing ability was evaluated by the DPV signals in the absence or presence of 100 pg mL^{-1} VEGF (Fig. 4A). After subtracting the similar blank signal, aptamer-hairpin probe 1 showed 3 times higher peak current than that of aptamer-hairpin probe 2, suggesting more effective sensing performance. The possible reason was that the primer hybridization site of aptamer-hairpin probe 1 was distant from GE surface, which reduced the steric hindrance for primer extension. So, the aptamer-hairpin probe 1 was chosen as the optimum probe in the experiments.

The target binding of aptasensor was sensitively dependent on different surface densities of aptamer due to conformational effects. As shown in Fig. 4B, the peak current increased with the

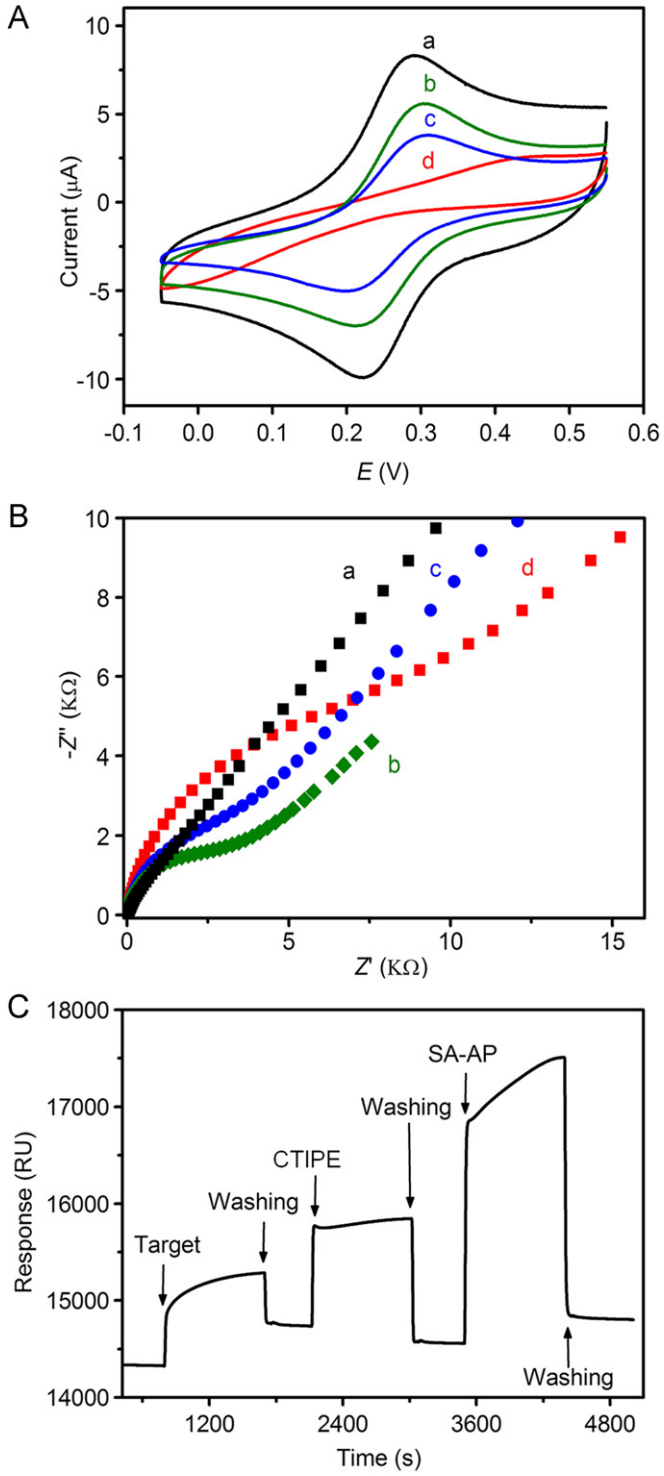

Fig. 2. (A) Cyclic voltammograms and (B) EIS of bare GE (a), aptamer-hairpin probe modified GE (b), aptamer-hairpin probe/MCH modified GE (c) and aptamer-hairpin probe/MCH modified GE after reaction with 1 ng mL^{-1} VEGF (d) in 0.4 M KCl containing 0.5 mM $[Fe(CN)_6]^{3-/4-}$ at 100 mV s^{-1}, and (C) SPR sensorgram of aptamer-hairpin probe/MCH modified chip upon successive treatments.

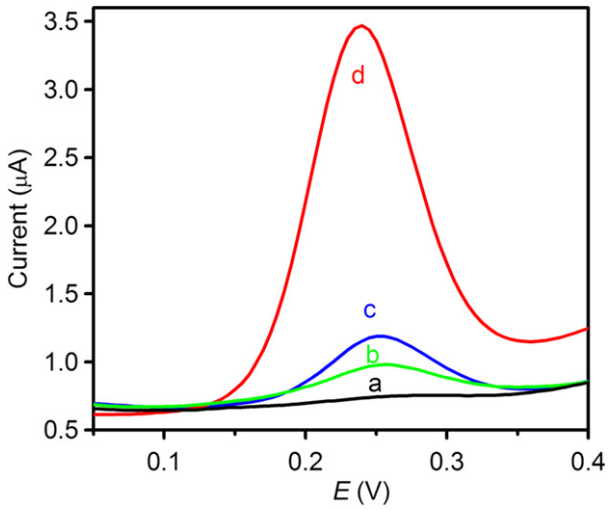

Fig. 3. DPV curves of designed aptasensor responding to 0 (a, b) and 100 (c, d) pg mL^{-1} VEGF without (a, c) and with (b, d) CTIPE, respectively.

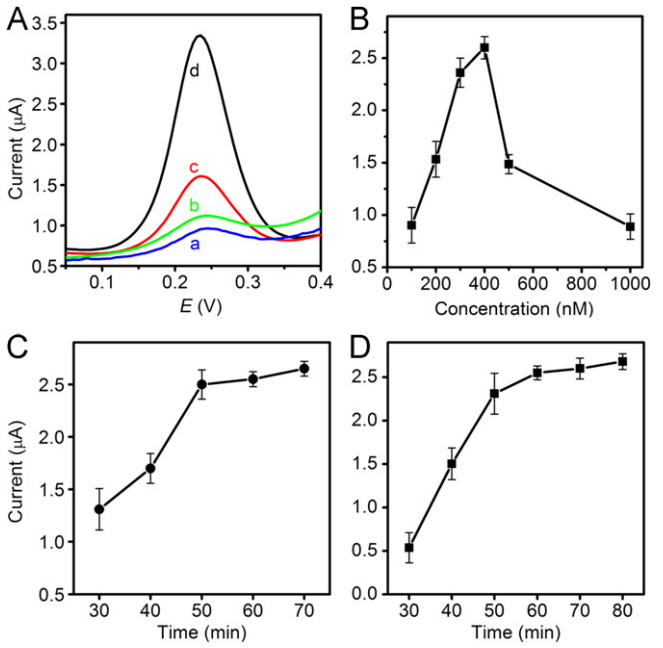

Fig. 4. (A) DPV curves of designed aptasensor responding to 0 (a, b) and 100 (c, d) pg mL^{-1} VEGF using aptamer-hairpin probe 1 (b, d) and 2 (a, c), respectively; and dependences of DPV signal on (B) aptamer-hairpin probe 1 concentration for aptasensor preparation, (C) incubation time with VEGF and (D) reaction time of CTIPE ($n=3$ for error bars).

increasing aptamer-hairpin probe concentration up to 400 nM for aptasensor preparation, due to the increased molecular coverage of aptamer-hairpin probe on the surface. Afterwards, the peak current decreased with the further increase of probe concentration, indicating that higher surface densities hindered the target binding and CTIPE process due to spatial restriction. So, the optimal incubation concentration of aptamer-hairpin probe was 400 nM.

With the increasing incubation time of VEGF the obtained peak current increased and tended to a steady value after 50 min, indicating a tendency to thoroughly capture target on the aptasensor surface (Fig. 4C). For sufficient binding of target protein, 60 min was chosen as the optimal incubation time. Similarly, a longer reaction time of CTIPE could generate more biotin-tagged DNA duplex for signal amplification due to the increasing cycle number, so the DPV response increased with the increasing reaction time (Fig. 4D). At 60 min the reaction reached saturation, which led to a constant signal. Thus 60 min was used for the CTIPE process.

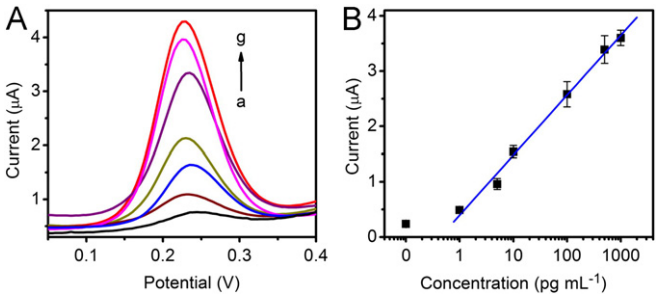

Fig. 5. (A) DPV curves of designed aptasensor responding to 0, 1, 5, 10, 100, 500, and 1000 pg mL^{-1} VEGF (a–g), and (B) quantitative dynamic range (n=3 for error bars).

Table 1
Assay results of practical specimens using the proposed and reference methods.

Sample no.[a]	1	2	3	4	5	6
Proposed method (pg mL^{-1})	930.4	499.9	174.2	1835.9	53.6	5.6
Reference method (pg mL^{-1})	1061.6	454.8	180.3	1991.7	51.3	–[b]
Relative error (%)	−12.3	9.9	−3.4	−7.8	4.5	–

[a] 1–3 Were serum samples, 4 and 5 were cell culture supernatants, 6 was 10 times dilution of sample 5. All the samples were diluted at 2 times prior to assay.
[b] Undetectable by reference ELISA method.

3.5. Analytical performance of designed aptasensor

Under optimal conditions, the DPV peak current increased with the increasing concentration of target protein (Fig. 5A). The plot of the response vs. the logarithm of target concentration showed a linear relationship in the detected range from 1 pg mL^{-1} to 1 ng mL^{-1} with a linear correlation coefficient of 0.997 (Fig. 5B). The limit of detection was calculated to be 0.82 pg mL^{-1} (17 fM) in a 3σ rule. Compared to fluorescent aptasensors based on isothermal strand-displacement polymerization (He et al., 2010; Qiu et al., 2011), the proposed electrochemical aptasensor showed a much lower limit of detection due to low blank signal and dual signal amplification of CTIPE and enzymatic catalysis. The limit of detection was also remarkably lower than those of electrochemical aptasensors using nanoparticle-based signal amplification strategy (Cheng et al., 2010a,b; Kara et al., 2010; Kuang et al., 2010; Zhou et al., 2010; Bai et al., 2011; Li et al., 2011), and comparable with those of electrochemical methods by aptamer-based RCA (Zhou et al., 2007) and scanometric strategies based on aptamer-initiated RCA (Cheng et al., 2010a,b). More importantly, such a performance was obtained without complicated preparation of biofunctional nanomaterials and circular DNA templates.

To estimate the reproducibility of the developed electrochemical aptasensor, the intra-assay imprecision of five different aptasensors at one assay and inter-assay imprecision at five different assays for detection of 100 pg mL^{-1} VEGF were examined, respectively. The intra-assay peak currents differed by 6.8%, and the coefficient of variation of interassay peak current was 11.4%. Thus the precision and reproducibility of the proposed electrochemical aptasensor was acceptable.

3.6. Detection VEGF in complex biological specimens

To further evaluate the analytical reliability and application potential, the proposed aptasensor was used to detect VEGF with a wide range of concentration in serum specimens and cell culture supernatants, and compared with the standard ELISA method, respectively. As shown in Table 1, the results obtained using proposed aptasensor were in good agreement with those obtained by the conventional ELISA method with relative errors from −12.3% to 9.9%. Thus, interference components in samples had little effect, and the designed method allowed accurate quantification of target protein in complex biological specimens without visible matrix effect. Moreover, the proposed aptasensor could quantitatively detect low-abundance VEGF in diluted cell culture supernatant, showing higher sensitivity than conventional ELISA method.

4. Conclusions

This work has demonstrated an ultrasensitive electrochemical aptasensor for convenient detection of protein by designing an aptamer-hairpin probe for target binding and integrating a versatile cyclic target-induced primer extension strategy and enzymatic electrochemical readout for dual signal amplification. The CTIPE strategy demonstrates remarkable amplification performance by transition of a single VEGF/aptame binding event to a lot of biotin-tagged DNA duplex. The designed aptasensor does not require thermal cycling and complicated preparation of circular DNA template and biofunctional nanomaterials, and shows an ultra-high sensitivity, acceptable reproducibility and a low matrix effect. The method has the potential for multiplex detection by designing more target-specific aptamer-hairpin probes for electrochemical sensor array. We anticipate that this method can be expanded readily as a simple and powerful tool for bioanalysis and clinic diagnostic application.

Acknowledgments

This work was funded by National Basic Research Program of China (2010CB732400) and National Natural Science Foundation of China (21075141, 21135002, 81101638 and 21121091).

References

Bai, L., Yuan, R., Chai, Y., Yuan, Y., Zhuo, Y., Mao, L., 2011. Biosensors and Bioelectronics 26, 4331–4336.
Carpini, G., Lucarelli, F., Marrazza, G., Mascini, M., 2004. Biosensors and Bioelectronics 20, 167–175.
Cheng, G., Shen, B., Zhang, F., Wu, J., Xu, Y., He, P., Fang, Y., 2010a. Biosensors and Bioelectronics 25, 2265–2269.
Cheng, W., Ding, Lin., Chen, Y., Yan, F., Ju, H.X., Yin, Y.B., 2010b. Chemical Communications 46, 6720–6722.
D'Orazio, P., 2011. Clinica Chimica Acta 412, 1749–1761.
Ellington, A.D., Szostak, J.W., 1990. Nature 346, 818–822.
Ferrara, N., Gerber, H.P., LeCouter, J., 2003. Nature Medicine 9, 669–676.
He, J.L., Wu, Z.S., Zhou, H., Wang, H.Q., Jiang, J.H., Shen, G.L., Yu., R.Q., 2010. Analytical Chemistry 82, 1358–1364.
Hianik, T., Ostatná, V., Sonlajtnerova, M., Grman, I., 2007. Bioelectrochemistry 70, 127–133.
Hianik, T., Wang, J., 2009. Electroanalysis 21, 1223–1235.
Kara, P., Escosura-Muñiz, A., Costa, M.M., Guix, M., Ozsoz, M., Merkoçi, A., 2010. Biosensors and Bioelectronics 26, 1715–1718.
Kuang, H., Chen, W., Xu, D., Xu, L., Zhu, Y., Liu, L., Chu, H., Peng, C., Xu, C., Zhu, S., 2010. Biosensors and Bioelectronics 26, 710–716.
Lai, R.Y., Plaxco, K.W., Heeger, A.J., 2007. Analytical Chemistry 79, 229–233.
Lee, J., Icoz, K., Roberts, A., Ellington, A.D., Savran, C.A., 2010. Analytical Chemistry 82, 197–202.
Liu, J., Cao, Z., Lu, Y., 2009. Chemical Reviews 109, 1948–1998.
Li, X.M., Li, W., Zhang, S.S., 2010. Analyst 135, 332–336.
Li, Y., Bao, J., Han, M., Dai, Z., Wang, H., 2011. Biosensors and Bioelectronics 26, 3531–3535.
Peng, Y., Zhang, D., Li, Y., Qi, H., Gao, Q., Zhang, C., 2009. Biosensors and Bioelectronics 25, 94–99.
Perez, J.M., Josephson, L., O'Loughlin, T., Hoegemann, D., Weissleder, R., 2002. Nature Biotechnology 20, 816–820.
Potty, A.S.R., Kourentzi, K., Fang, H., Jackson, G.W., Zhang, X., Legge, G.B., Willson, R.C., 2009. Biopolymers 91, 145–156.
Prabhulkar, S., Alwarappan, S., Liu, G., Li, C.Z., 2009. Biosensors and Bioelectronics 24, 3524–3550.
Qiu, L.P., Wu, Z.S., Shen, G.L., Yu, R.Q., 2011. Analytical Chemistry 83, 3050–3057.
Sassolas, A., Blum, L.J., Leca-Bouvier, B.D., 2009. Electroanalysis 21, 1237–1250.
Tombelli, S., Minunni, M., Mascini, M., 2005. Biosensors and Bioelectronics 20, 2424–2434.

Wang, J.L., Zhou, H.S., 2008. Analytical Chemistry 80, 7174–7178.
Wang, J., Meng, W., Zheng, X., Liu, S., Li, G., 2009. Biosensors and Bioelectronics 24, 1598–1602.
Xu, Y., Cheng, G., He, P., Fang, Y., 2009. Electroanalysis 21, 1251–1259.
Yoshizumi, J., Kumamoto, S., Nakamura, M., Yamana, K., 2008. Analyst 133, 323–325.
Zhang, H.Q., Zhao, Q., Li, X.F., Le, X.C., 2007. Analyst 132, 724–737.
Zhang, S., Hu, R., Hu, P., Wu, Z.S., Shen, G.L., Yu, R.Q., 2010. Nucleic Acids Research 38, e185.
Zhao, W., Ali, M.M., Brook, M.A., Li, Y., 2008. Angewandte Chemie—International Edition 47, 6330–6337.
Zhou, J., Huang, H., Xuan, J., Zhang, J., Zhu, J.J., 2010. Biosensors and Bioelectronics 26, 834–840.
Zhou, L., Ou, L.J., Chu, X., Shen, G.L., Yu, R.Q., 2007. Analytical Chemistry 79, 7492–7500.
Zuo, X., Song, S., Zhang, J., Pan, D., Wang, L., Fan, C., 2007. Journal of the American Chemical Society 129, 1042–1043.